Brillouin Fiber Laser Pumped by a DFB Laser Diode

Jae Chul Yong, Luc Thévenaz, *Member, IEEE*, and Byoung Yoon Kim, *Fellow, IEEE*

***Abstract*—In this paper, we present a novel Brillouin fiber-ring laser utilizing an unbalanced Mach–Zehnder interferometer (UMZI) as coupling device. The laser is pumped by a distributed-feedback laser diode and shows continuous-wave and single-frequency operation. Frequency-dependent transmission characteristics of the UMZI make it possible for the pump wave to pass through the laser-ring cavity with no resonance effect for stable pump operation, while the Brillouin laser signal still resonates in a high-finesse cavity. Single and multiple longitudinal mode operations are observed according to the relative location between longitudinal modes and Brillouin gain-curve center. A stable single-frequency operation is achieved using a simple stabilizing feedback loop based on dithering and autotracking techniques. Using this simple stabilizing feedback loop, the laser-intensity fluctuation is highly suppressed and remains below 4%. The Brillouin output converted from the pump power of 26.4 mW is about 3.18 mW, and the linewidth is measured to be below 1 kHz.**

***Index Terms*—Brillouin scattering, optical-fiber devices, optical-fiber lasers, optical resonators.**

I. Introduction

STIMULATED Brillouin scattering (SBS) is a nonlinear effect resulting from the interaction between intense pump light and acoustic waves in a medium and giving rise to backward propagating frequency-shifted light [1]. The mechanism of SBS is the following: thermally excited acoustic waves generate an index grating that copropagates with the pump at the acoustic velocity in the material. This moving grating reflects the pump light and causes this backscattered light (Stokes wave) to be downshifted in frequency through the Doppler effect. This process can be stimulated when the interference between the counterpropagating pump and Stokes waves reinforces the acoustic wave through the action of electrostrictive forces. Electrostriction represents the tendency of materials to densify in regions of high optical intensity. In particular, SBS can easily take place in an optical fiber as a result of its small core diameter and low loss and requires the lowest power to be observed among all nonlinear phenomena in fibers. The frequency shift with respect to the pump is given by $\Delta\nu_{\mathrm{BS}} = (2V_A/c)\nu_P$, where V_A is the acoustic velocity in the medium, c is the vacuum-light velocity, and ν_P is the optical frequency of the pump beam. Typical values of the frequency shift in single-mode fibers (SMFs) range from 9.5 to 11.5 GHz in the 1.55-μm wavelength region, depending on the fiber materials and structure [17].

Although Brillouin generation can be detrimental in coherent optical-communication systems [2], [3], it has been advantageously utilized in the past few years for the following applications: a) optical-fiber characterization [4], [5]; b) distributed attenuation measurements along an optical link [6]; c) distributed strain and temperature measurements [7], [8]; d) narrow-bandwidth amplification [9]; e) frequency shifter [10]; and f) microwave-frequency generation [11]. Perhaps the largest interest has arisen from the use of SBS to produce Brillouin fiber lasers [12]–[14] with applications such as gyroscopes [15].

In this paper, we examine the use of SBS for Brillouin fiber lasers (BFLs). BFLs have generated interest for a number of applications owing to their extremely narrow linewidth [16]. The key features of BFLs for most applications are the very high coherence and the directional sensitivity of the SBS gain. The bandwidth of Brillouin gain is very narrow, typically from 20 to 50 MHz for wavelengths in the near infrared, but its magnitude is fairly small [17]. Thus, BFLs are generally constructed in an all-fiber, high-finesse ring-resonator arrangement [14] to achieve low laser threshold and efficient operation. Submilliwatt thresholds [13] are easily achievable if the pump signal coincides with one of the resonator modes. For a maximum pump intensity circulating in the resonator, not only the launched polarization state must match an eigenpolarization of the ring resonator, but also the frequency of pump must track a cavity resonance through a servo loop. The servo loop for frequency locking of the pump wave to a resonant frequency of the fiber-ring resonator is usually based on an FM sideband technique [18]. Good internal conversion efficiency over 50% can be achieved [19], but high-finesse resonator results generally in small output power. While excellent performance can be achieved from BFLs in terms of linewidth, the narrow bandwidth and small gain coefficient of the Brillouin gain generally require resonator designs that include active stabilization for efficient stable resonator.

For laser oscillation, closed-loop gain must exceed unity so that Brillouin amplification must overcompensate the cavity loss. As a result of the small SBS linear gain, a cavity length of several meters is required to obtain threshold powers in the milliwatt range. But long cavities result in narrow resonance in the frequency domain and sub-Megahertz linewidth of cavity modes is observed as soon as the cavity length exceeds a few meters. This makes the spectrum of a standard distributed-feedback (DFB) laser diode impossible to fit into a cavity resonance, decreasing drastically the circulating pump intensity and causing large fluctuations of the pumping power

Manuscript received March 7, 2002.

J. C. Yong was with the Department of Physics, Korea Advanced Institute of Science and Technology, Taejon, 305-701, Korea. He is now with FiberPro, Taejon 305-301, Korea (e-mail: jcyong@fiberpro.com).

L. Thévenaz is with the Laboratory of Metrology and Photonics, Swiss Federal Institute of Technology, Lausanne CH-1015, Switzerland (e-mail: Luc.Thevenaz@epfl.ch).

B. Y. Kim is with the Department of Physics, Korea Advanced Institute of Science and Technology, Taejon 305-701, Korea.

Digital Object Identifier 10.1109/JLT.2003.808768

through phase noise. So far, this has made the laser diode incompatible with the requirements for pumping a BFL.

Recently, Cowle *et al.* [20] proposed a hybrid Brillouin/erbium fiber laser. In the novel mode of operation for a BFL, they overcome the need for a critically coupled resonator in a laser based on Brillouin gain by using an erbium-doped fiber (EDF) amplifier to compensate for the resonator losses, while still originating lasing action from the Brillouin gain. Moreover, the combination of two gain media, the gain from the EDF and Brillouin gain in single mode fibers allows a resonator to support a laser comb with ~10 GHz spacing at room temperature. However, because two gain media are used in this case, fine control of each gain profile is required and the optical configuration is complex. An optical isolator severely increasing the cavity loss is needed to prevent depletion of the gain by the injected signal and injection locking to the Brillouin pump.

In this paper, we propose and demonstrate a novel BFL pumped by DFB laser diode (LD), with advantages of simple configuration and no need for cavity matching of the pump frequency. In this work, we overcame the requirement of a critically coupled resonator in a BFL by using an unbalanced Mach–Zehnder interferometer (UMZI) instead of a coupler and high power DFB LD as a pump source. Brillouin generation in SMF requires a pump with sufficient power to reach threshold, and with linewidth less than the Brillouin gain bandwidth for good efficiency. So far, it is difficult to utilize a DFB LD for a Brillouin pump due to its broad linewidth (from order of submegahertz to megahertz) compared to the bandwidth (a few tens kHz) of the high-finesse ring-resonator cavity, resulting in output power instability. Nowadays, DFB LD technology supports a pump source with output power >10 mW and spectral width ~1 MHz, which can be successfully applied to the Brillouin pump source in the configuration with the UMZI. The Brillouin pump is required for the onset of laser operation, but is not resonant in the laser cavity. At the Stokes wavelength, the BFL operates in a single longitudinal mode, the cavity mode spacing being comparable to the Brillouin gain linewidth. Since this scheme enables the BFL to use a commercial DFB LD for a pump source, the structure of BFL can be compact and robust. In addition, a high-finesse cavity is preserved for Brillouin emission in such a configuration. The ring topology and narrow linewidth of the BFL may be attractive for sensor applications such as laser gyroscope [15] and electrical-current monitors [21]. Other applications of this method include linewidth-narrowing of many other lasers.

This paper explores some fundamental aspects of BFL using an UMZI configured to generate a stable single frequency. Section II contains an operating principle of the laser, including spectral characteristics of the UMZI and instability problems. Experimental results are reported in Section III. Proof of single longitudinal mode operation, linewidth measurement, and power stability are described. Section IV is devoted to the conclusion.

II. Operating Principle

In this section, a novel Brillouin laser configuration using a UMZI for stable laser-output power is described. In order to obtain an efficient BFL with stable output power, pump source must be stable in optical frequency as well as in power. Furthermore, it is desirable that the laser cavity satisfies simultaneously the following requirements.

1) Pump light must pass through the cavity with only one roundtrip, so that it is not resonant in the cavity and its spectrum must not fit within a cavity mode.
2) SBS light must circulate in the cavity with multiple roundtrips and experience little loss, so that it benefits from the resonance cavity for efficient lasing action.

Here, we will further demonstrate that these requirements can be fulfilled using an UMZI instead of a single coupler used in a conventional ring-resonator configuration.

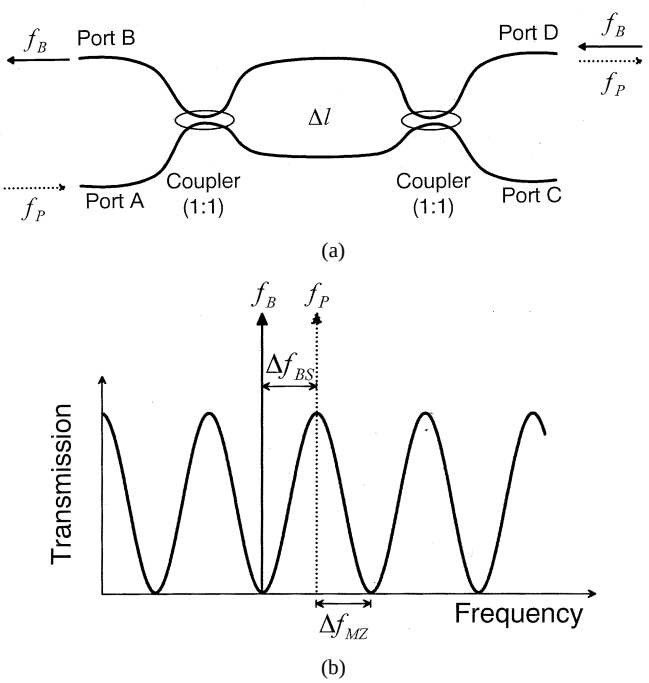

Fig. 1. (a) Unbalanced MZ fiber interferometer and (b) its transmission spectrum. f_P and f_B represent the ideal spectral positioning of pump and Brillouin emissions, respectively.

A. Unbalanced MZ Interferometer (Filter)

Fig. 1(a) shows a schematic diagram of an UMZI made of two fiber couplers with power-splitting ratios as close as possible to 50%. Our configuration fully takes advantage of the property that the UMZI responds differently to light at different frequency. Assuming that the UMZI has neither loss nor birefringence, when a lightwave with optical frequency f is incident to port A, the normalized transmission T at port D is given by

$$T = \frac{1}{2}\left(1 + \cos\frac{2\pi n \Delta l}{c} f\right) \tag{1}$$

where n is the refractive index of the optical-fiber arms, Δl is the length difference between the two arms of the UMZI, and c is the velocity of light in vacuum. In the case of a given length difference Δl, the transmission spectrum (from port A to port D) of the UMZI is a periodic function of optical frequency f, as illustrated in Fig. 1(b). It can serve as a periodic filter with broad bandpass transmission. The frequency difference between

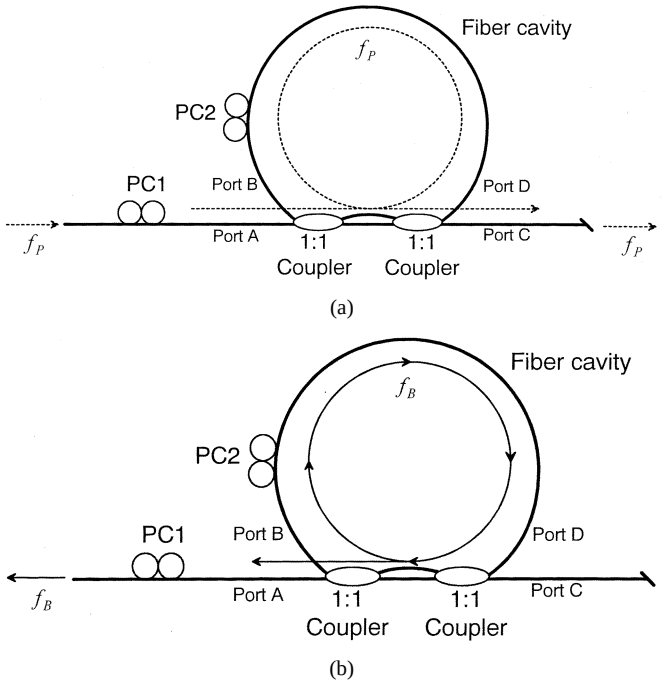

Fig. 2. Schematic diagram of a Brillouin fiber laser cavity employing an unbalanced MZ interferometer (PC1, 2: polarization controllers). (a) The pump propagates once through the cavity, while (b) the Brillouin emission makes multiple circulations.

maximum and minimum transmission Δf_{MZ} is determined by the optical-path difference (OPD) $n\Delta l$, and is given by

$$\Delta f_{\mathrm{MZ}} = \frac{c}{2n\Delta l}. \tag{2}$$

If an input (pump) light directed to port A has an optical frequency f_P [dotted line in Fig. 1(b)], it is totally coupled to port D. If a light of optical frequency f_B [solid line in Fig. 1(b)] is entered into a port D, it is coupled to port B with 100% efficiency as well.

Using these transmission characteristics of the UMZI, we can realize a compact Brillouin fiber laser cavity satisfying aforementioned requirements 1 and 2. Fig. 2 shows a configuration of BFL employing the UMZI. The topology of the laser is similar to a conventional Brillouin fiber-ring laser except that the UMZI is used instead of a coupler, precluding optical resonance of a pump light. The ports B and D are connected by an optical SMF which can give rise to SBS gain. An intense beam of light injected into the SMF, the pump, generates narrow-bandwidth gain in the clockwise direction, at a frequency shifted from the pump frequency by the Stokes shift (Δf_{BS}) in the SMF. The strong attenuation of sound waves in silica determines the shape of the Brillouin gain spectrum. Actually, the exponential decay of the acoustic waves results in a Lorentzian gain profile [1].

A pump light whose frequency f_P is matched with that of maximum transmission of Fig. 1(b) is coupled from port A to port D, and then propagates through the fiber cavity, and finally goes straight out of the cavity from port B to port C. This makes the pump circulate only once in the cavity, preventing any resonance effect. In the same way, the length difference between the two branches of the UMZI can be controlled, so that the frequency interval (Δf_{MZ}) is equal to the Brillouin shift Δf_{BS} as depicted in Fig. 1(b). Hence, the Stokes beam with frequency f_B traveling the cavity in a direction opposite the pump light experiences maximum transmission from port D to B and therefore circulates the cavity loop many times with small loss. Since the Brillouin shift of a conventional SMF at 1560 nm wavelength is about 10.8 GHz (87.5 pm), the corresponding length difference between the two branches of the UMZI must be about 9.52 mm. In summary, we can achieve the two requirements simply by controlling the frequency of pump light and the optical-path difference between the two arms of the UMZI. In an ideal situation, the UMZI serves as a 100% coupler for a pump beam and as a 0% coupler for a Brillouin signal.

However, in a real system using the proposed cavity configuration, the cavity fiber as well as the UMZI shows birefringence, thus, the transmission spectrum can vary with the state of polarization (SOP) of an input light. Therefore, it is necessary to insert two polarization controllers (PCs) in front of port A and in the loop cavity to properly set the SOP of pump light, as illustrated in Fig. 2. Calculations based on Jones matrix formalism conclude that, by controlling the SOPs at ports A and B and the frequency of pump light, requirement 1 (one roundtrip for pump light) is fulfilled. This can be simply achieved this way: 1) by using PC1, the SOP of pump at port A must be adjusted, such that light passing through each branch of the UMZI shows an identical SOP at port D for maximal interference; 2) by setting PC 2, the pump SOP at port B must be controlled to be equal to that at port A; and 3) the pump frequency should be tuned on the maximum transmission point of the UMZI. It should be mentioned that in this situation, the pump wave is automatically launched into the laser cavity (UMZI + fiber loop) along an eigenpolarization state.

On the other hand, the transmission of UMZI for the SBS light is determined by the eigenmode of the laser cavity, and therefore, depends on the birefringence of the laser cavity and UMZI. Furthermore, two orthogonal polarization eigenmodes have different transmission values. Of course, the smaller the difference of birefringence between the two arms of the UMZI is, the smaller the polarization dependence of the Brillouin laser cavity is. So care must be taken not to produce large stress-induced and bend-induced birefringence in the fibers forming the UMZI and the cavity. Finally, it must be noticed that the eigenpolarization state of the SBS signal is given by the complex conjugate of that of the pump, the laser cavity being full reciprocal and the small frequency difference between the pump and the Stokes waves being neglected [22].

B. Power Stability

In the case of a Brillouin laser using the UMZI, there are three major sources causing output power fluctuation. The first is frequency jittering and power fluctuation of pump LD itself. The frequency jittering especially can induce large power fluctuation because the transmission of the UMZI is dependent on the pump light frequency. In general, power and frequency of an LD depend on the current injected into the LD as well as the temperature of the LD. Therefore, it is essential to maintain the current and temperature of LD constant to grant a good power stability.

The second is variation of the optical-path difference of an UMZI due to environmental perturbation, especially ambient

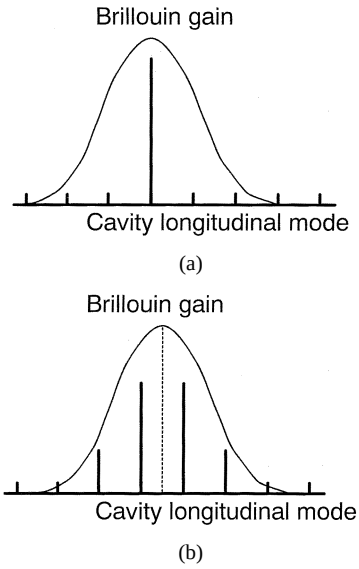

Fig. 3. Oscillating modes of a Brillouin fiber laser depend on the position of the cavity modes under the Brillouin gain spectrum: (a) single-mode operation and (b) multiple-mode operation.

temperature change, because the transmission spectrum of the UMZI is directly related to the optical path difference, as shown in (2). For instance, in the case of an UMZI with an optical-path difference of 1 cm, the transmission can be varied from maximum value 1 to 0.88 for a temperature change of 1 °C. For stabilizing the transmission of the UMZI within $\pm 1\%$ of the maximum transmission point (from 1 to 0.99), the temperature of the UMZI must be maintained within ± 0.3 °C. This experimental condition is not very severe, but thermal isolation and simple temperature control are nevertheless required.

If the pump frequency is deviated from the maximum transmission position due to these two effects, the pump power starts to resonate in the cavity and suffers from large fluctuations, like in the case of a conventional ring-resonator configuration, resulting in considerable laser-output power instability.

The third source of fluctuation is the drift of the laser frequency resulting from variations of the refractive index and of the length of a cavity fiber due to ambient temperature change. The oscillation frequency of the BFL is mainly determined by both the cavity resonances and the wavelength of the Brillouin pump. The longitudinal mode of the cold resonator located under the Brillouin gain curve that experiences the highest gain oscillates. The oscillation frequency is, therefore, temperature-dependent, since both free-spectral range (FSR) and the gain-curve center depend on the temperature. A temperature increase of the fiber-ring cavity induces both a reduction of the FSR and an increase of the Brillouin frequency shift (1.36 MHz/°C at 1.32 μm) [23]. The FSR variation gives rise to a continuous lasing frequency variation while the gain curve shift leads to mode hopping. If one of the laser-cavity modes matches well the center of Brillouin gain as illustrated in Fig. 3(a), the laser oscillates in single mode at the highest power. As the longitudinal mode is detuned from the gain center, the laser output decreases accordingly. Moreover, when the mode is detuned further, so that the gain center is located at the midpoint between the two adjacent longitudinal modes as shown in Fig. 3(b), the laser can oscillate in multiple longitudinal modes. Strictly speaking, the detuning range where the laser operates in multimode is essentially determined by pump power (that is, gain magnitude). It turns out that it is required to control the optical path length of cavity actively by using an electric feedback control to achieve stable single mode operation.

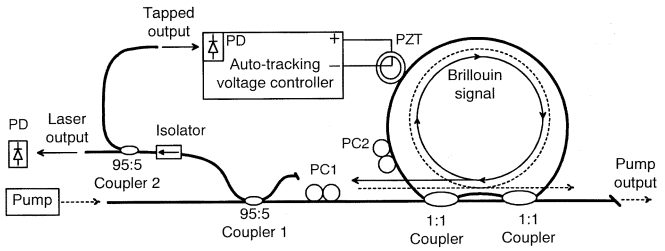

Fig. 4. Experimental setup of a Brillouin fiber laser using the unbalanced MZ fiber interferometer (PC1, 2: polarization controllers, PD: photo detector).

In summary, the power of the pump light must be kept constant and the lasing mode should be locked at the center of the Brillouin gain by some control, in order to make the lasing of the Stokes light as stable as possible.

III. Experimental Results

A. Experimental Setup

Fig. 4 shows the experimental setup of the Brillouin fiber laser based on an UMZI. In the figure, pump light and SBS light are represented by dashed line and solid line, respectively. The UMZI was built using two fused-fiber couplers, showing splitting ratio of 49.7%:50.3% and 51.1%:48.9% and the losses were 2.3% and 1.2%, respectively. Omitting the birefringence of the UMZI, the minimum transmission is expected to be -42.1 dB. We spliced the two arms of each coupler while managing to make the length difference between the two branches of the UMZI 9.52 mm ($\Delta f_{\mathrm{MZ}} = 10.8$ GHz), which corresponds to the Brillouin shift of the SMF at 1560 nm. At room temperature, the actual frequency difference Δf_{MZ} of the UMZI was measured to be 86.8 pm (10.7 GHz) by using an optical spectrum analyzer and a broadband source. The transmission function of the UMZI showed some polarization sensitivity due to birefringence in the fiber and the minimum transmission was measured to below -25.8 dB over most launched states of polarization. Because of this imperfect minimum (maximum) transmission value, the pump power in the cavity depends on the accumulated phase of the pump light during one round trip through the interference effect. While the minimum transmission is pretty small $(-25.8\ \mathrm{dB})$, the pump-power variation can be about 20% due to the resonant behavior of the interference assuming that the pump source is perfectly coherent. Fortunately, however, the linewidth of a commercial LD is limited to a few megahertz (corresponding coherence length: a few tens meters) and the cavity length is longer than a few tens of meters, so that the pump-power variation can be significantly reduced to a few percents.

For temperature stability of the UMZI, it was packaged into an aluminum case that was temperature-controlled using a thermo-electric cooler. The temperature stability was observed

to be better than 0.04 °C after 16 h monitoring of the UMZI output. During this measurement, the ambient temperature changed by 1.1 °C. Attention must be paid to the fact that the optical-path difference of the UMZI can be adjusted finely by changing the temperature of the UMZI, so that the frequency difference Δf_{MZ} is well matched to the Brillouin shift Δf_{BS}. Since the Brillouin shift depends on the fiber characteristics, a tuning capability of the UMZI is important for practical realization. The laser cavity, forming the gain medium, was made of a 27.6-m-long SMF (Corning SMF-28) that was spliced to two opposite ports of the UMZI. A portion of the cavity fiber was wound around a cylindrical piezoelectric transducer (PZT) to be used as a cavity-length controller.

As pump source, we used a 1559.6-nm DFB LD (maximum power: 50 mW) with a built-in optical isolator. As mentioned in Section II-B, it is important to reduce fluctuations of current and temperature of the DFB LD for stable single-mode operation of the Brillouin laser. To properly estimate the impact of supply noise, we measured current and temperature dependence of the LD frequency. The results are -0.215 GHz/mA at temperature of 25 °C and -11.1 GHz/°C at pumping current of 150 mA, respectively. While most of commercial current controllers have small ripple noise (from a few tens to a few hundreds μA), this small noise results in frequency jitters of the LD from several to several tens MHz, which is enough to cause large fluctuations of output power in the case of a Brillouin laser. The ripple is mainly 60-Hz noise (or harmonics of 60 Hz) resulting from an imperfect rectification of the ac power line and pick-up in the current controller. To suppress the 60-Hz current ripple, we have developed a battery-powered current supply. For the case of temperature controller, we cannot find any serious problem in the use of a commercial temperature controller.

The pump beam was launched into the laser cavity through the 95:5 coupler 1. This coupler also acts as tapping for the SBS light output propagating in the opposite direction to the pump beam. The SBS output was then split again by another coupler (95:5 coupler 2). One branch is used for laser output and the other for providing an error signal to the cavity-length feedback.

To prevent the frequency drift of the laser modes that results in power fluctuation and multimode operation, we implemented an autotracking feedback loop, which actively matched one longitudinal mode with the center of the Brillouin gain spectrum. To control the optical-path length of the cavity that is directly related to the frequency of the longitudinal modes, we applied an autotracking control voltage to the cylindrical PZT. The main principle of the autotracking is a classical dithering method. The voltage applied to the PZT is dithered, so that the frequency of the lasing mode changes accordingly. By analyzing the laser output during the dithering, the applied voltage was controlled in such a way that the laser power was maximized, an consequently, the laser mode tracked the gain center. An optical isolator was inserted between the two 95:5 couplers for preventing re-entry of back-reflected laser output into the cavity, which may destabilize the laser output. The total cavity (UMZI and fiber loop) was placed into a styrofoam box for reducing environmental perturbations.

In order to find the proper operating conditions fulfilling the requirements stated in Section II, we first controlled the frequency and polarization of the pump DFB LD at a preset current level below the BFL threshold by adjusting the temperature of LD and the PC 1 located at the input port, in such a way that the power to pump output port was minimized. During this procedure, we blocked the laser cavity by using bending loss of the fiber to remove interference effect due to multiple pump roundtrips. Next, we released the bending and controlled the SOP of pump light in the cavity loop by using the PC 2 so that the power to pump output port was maximized and simultaneously the interference effect resulting from pump multiple circulations was minimized. These procedures guarantee that the laser cavity satisfies requirement 1. Once, after finding the proper condition, we could freely increase the pumping current of the LD above BFL threshold. Of course, we had to change the temperature of the LD simultaneously so that the frequency of the pump light is located at the maximum transmission point of the UMZI. Since the polarization properties of the Brillouin laser cavity did not change noticeably for such a small optical-frequency change (below a few tens GHz), we did not need to optimize the SOP of pump source repetitively during the increase of the pumping current.

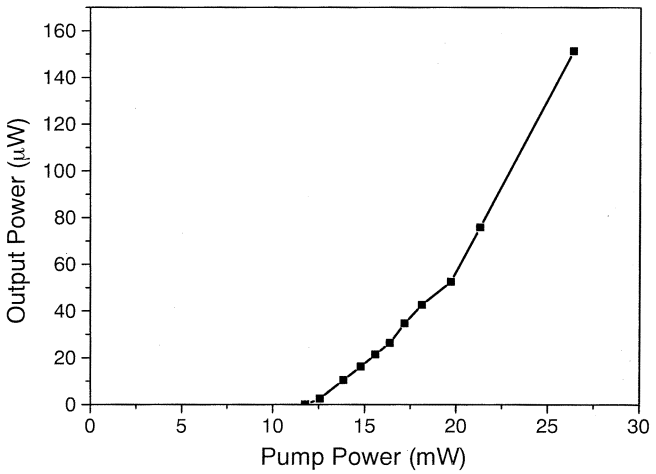

Fig. 5. Brillouin laser-output power as a function of pump power.

B. Threshold and Output Power

In the following the characteristics of the Brillouin laser output including threshold, output power, mode spectrum, and stability are described.

Fig. 5 shows the Brillouin laser-output power as a function of the pump power. Pump power was measured directly at the DFB LD fiber pigtail and Brillouin laser output was measured at the 95% port of the 95:5 coupler 2. When the pump power is increased through the current applied to the DFB LD, the temperature was also changed in order to tune the frequency of LD for a proper operation condition. As shown in Fig. 5, the output power is proportional to the pump power as expected. However, it does not show a clear linearity. This results from the fact that we could not control the frequencies of the DFB LD with the same accuracy through all measurements. For instance, we observed that for a 1 mA pumping current change, the output power could be increased by 51% if the DFB LD temperature is maintained constant. An accurate proper setting was therefore

very difficult to obtain and minor inaccuracies may account for the shifts from linearity observed in Fig. 5.

The threshold was about 11.8 mW (pumping current = 91 mA). Since SBS originates from the coherent mixing between pump and Stokes waves, the Brillouin gain depends on the relative polarizations of the pump and of the Stokes wave [22]. A maximum gain in BFL is obtained when the polarization of the pump is kept parallel to that of the Stokes wave. For determining the overall Brillouin gain after one roundtrip, it is essential to analyze the eigenstates of polarization for the pump and the Stokes wave along the fiber-ring resonator. Although some characteristics of the eigenstates are described in Section II-A, the full analysis of the eigenpolarization and effective gain is beyond the scope of this paper. The detailed analysis can be found in [22] and [24]. For polarization maintaining fibers, intuitively, the Brillouin gain is maximum for parallel linear polarization aligned to a birefringence axis and 1/2 for linear polarization launched at 45° of the birefringence axis. However, Deventer *et al.* [25] showed that the situation is entirely different for low-birefringence fibers. The effective gain is decreased due to pump and Stokes wave polarization mismatch along the fiber, provided that the fiber length exceeds a few birefringence beat length and when the polarization is not preserved. The overall gain in low-birefringence fibers with random polarization change ranges from 1/3 to 2/3 of its maximum value for the best polarization matching. From the threshold value and effective Brillouin gain, total cavity loss (including output coupling) for SBS light was calculated to be about 8% if the polarization of the pump is well matched with that of the SBS wave through the entire cavity, and 5% if the pump is randomly polarized with respect to polarization of the SBS wave due to cavity birefringence.

At the pumping power of 26.4 mW, the laser-output power was 151 μW. Considering the coupling ratios of the two tapping couplers (95:5 coupler 1 and 2), SBS output power from the UMZI converted from the pump power with the help of Brillouin amplification process is about 3.18 mW.

C. Mode Spectrum

The Brillouin laser could operate in continuous wave (CW) single mode as well as in pulsed multimode emission depending on the relative cavity and Brillouin gain spectrum condition. Fig. 6 shows RF spectra of the beat signal between the pump light and Brillouin laser output measured with a high-speed photoreceiver and an RF spectrum analyzer. We have combined each other using a 50:50 coupler to produce the interference. This set of measurements was performed on another Brillouin laser cavity made of 34.0 m of standard single mode fiber (free spectral range = 6.5 MHz). The threshold power was in this case 17.9 mW and the operation pumping power was 30.8 mW. Only one frequency component can be observed in Fig. 6(a) at 10.787 GHz, corresponding to the Brillouin shift of the fiber, indicating single-mode operation. However, in Fig. 6(b), there are multiple frequency components over the entire gain bandwidth (about 20 MHz), spaced by the free spectral range of the laser cavity and indicating multimode operation. In this case, several longitudinal modes of the resonator were spontaneously

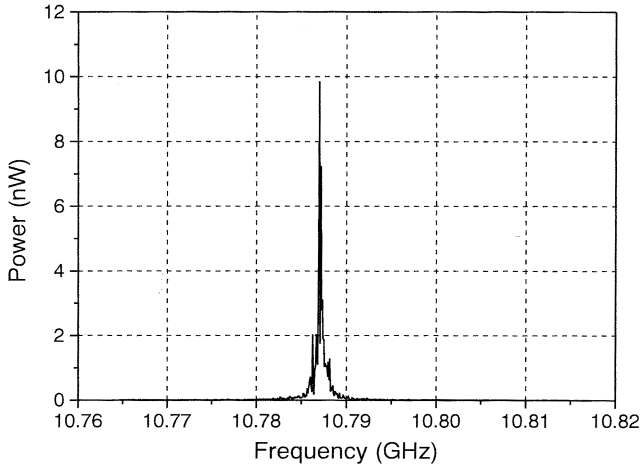

(a)

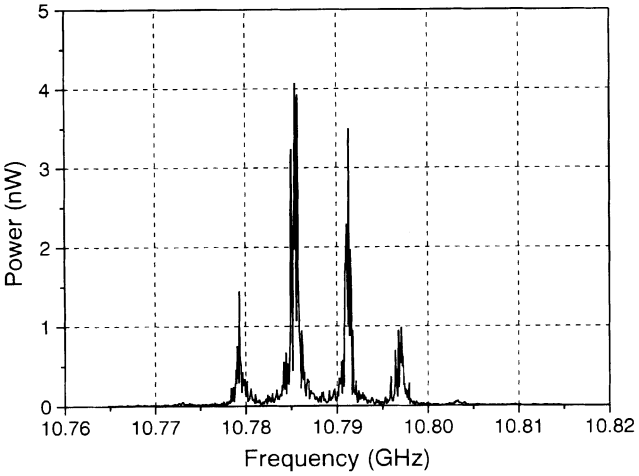

(b)

Fig. 6. RF spectra of the beat signal between the pump and the Brillouin laser output: (a) single-mode operation and (b) multimode operation.

mode-locked and therefore, the laser output was pulsed, as observed in the time domain. The mode locking mechanism may be related to periodic pump depletion in the Brillouin medium caused by external feedback into the cavity but is not fully understood to date [26]. Alternation between single and multiple mode operation can be explained by the frequency difference between longitudinal modes and Brillouin gain center as discussed in Section II-B. We have focused on the single mode operation in this work. The detailed description of the multimode operation is beyond the scope of this paper.

Fig. 7 shows mode spectra of the pump DFB LD and Brillouin laser output monitored by a scanning fiber-ring resonator (Resolution: 0.6 MHz, free spectral range: 70 MHz). In both pictures, the triangular waveform represents the scanning voltage applied to the fiber-ring resonator. The pump DFB LD was operated in a single-frequency mode with a 2.9-MHz linewidth, as illustrated in Fig. 7(a). Fig. 7(b) shows the spectrum of the Brillouin laser output, indicating single mode operation. Comparing Fig. 7(a) with Fig. 7(b), the linewidth-narrowing effect of Brillouin lasing is evident. The linewidth of the laser output was below 0.6 MHz, that is the resolving limit of the scanning fiber-ring resonator.

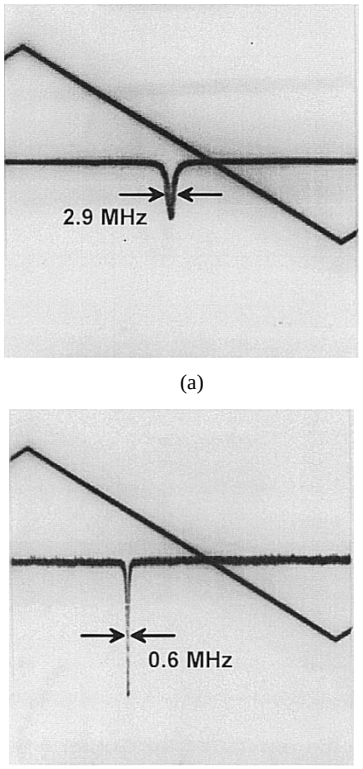

Fig. 7. Laser-mode spectra monitored by a scanning fiber-ring resonator (resolution: 0.6 MHz): (a) pump laser diode and (b) Brillouin laser.

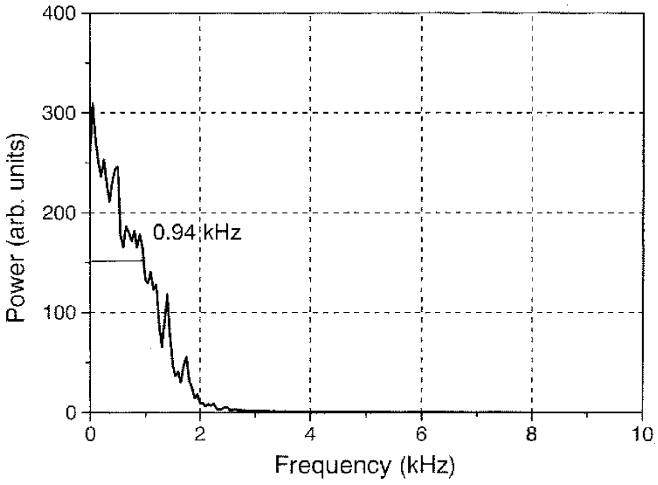

Fig. 8. Self-homodyne measurement of the Brillouin laser linewidth using a 20-km delay line. The resolution bandwidth of the RF spectrum analyzer is 150 Hz and the sweep time is 3.28 s.

To measure the linewidth of the laser output more accurately, a self-homodyne detection technique was realized using a MZ interferometer with a 20-km optical-fiber delay line, corresponding to a delay time of 97 μs. Fig. 8 shows the interference output signal detected by a photodetector and an RF spectrum analyzer. The spectrum was averaged over 50 3.28-s samples with a 150-Hz resolution bandwidth. The observed linewidth of the spectrum is 0.94 kHz, which corresponds to a coherence time of 339 μs. Because this coherence time is greater than the delay time, we can conclude that the optical linewidth of the laser is below 0.94 kHz [27].

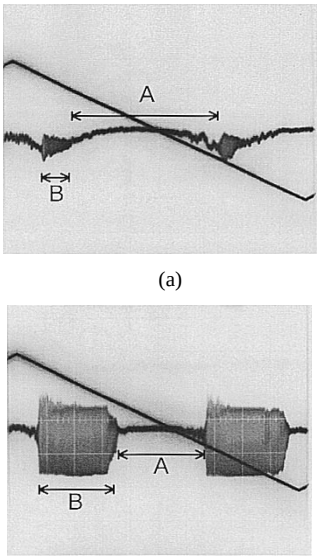

Fig. 9. Laser output variation when the longitudinal modes are scanned over more than the free spectral range of the cavity: (a) pump power 15.4 mW and (b) pump power 18.8 mW. Zone A represents the single-mode region and Zone B the multimode region.

D. Stability

As illustrated in Fig. 3(a) and (b), the power and the number of oscillating modes of the Brillouin laser are dependent on the position of the Brillouin gain profile with respect to longitudinal modes. To examine this behavior in detail, we scanned the frequencies of the longitudinal modes of the laser cavity by using the cylindrical PZT modulator. Fig. 9 shows laser output variation monitored by a high-bandwidth (125 MHz) photodetector when we applied triangular waveform voltage to the PZT. The frequency scan was larger than the FSR of the cavity. The pump power was 15.4 and 18.8 mW for Fig. 9(a) and (b), respectively. In region A, the laser operates in single mode and the power is changed according to the frequency detuning between Brillouin gain and cavity modes. In region B, the output power baseline is broadened as a result of the beat between lasing modes, indicating pulsed multimode operation. This result supports the fact that lasing mode is a function of the relative location between the axial modes and the gain curve center. This strongly suggests that the regions A and B correspond to the situations of Fig. 3(a) and (b), respectively. Comparing Fig. 9(a) and (b), the multimode region is widened in proportion to the pump power as can be expected intuitively.

In a real environment, the Brillouin laser can switch from single-mode to multimode operation randomly and the power can fluctuate as well due to ambient temperature change causing the drift of laser-mode frequency. For stable single-mode operation, it is therefore required that one particular longitudinal mode well matches the gain-center frequency and that this condition is permanently maintained. This could be fulfilled by controlling the optical-path length of the laser cavity in such a way that the laser mode follows the gain center by utilizing a dithering and autotracking method. Fig. 10 shows the laser-output power drift for 20 min. The power fluctuation was less than 4% when the autotracking was turned on. The pump-power

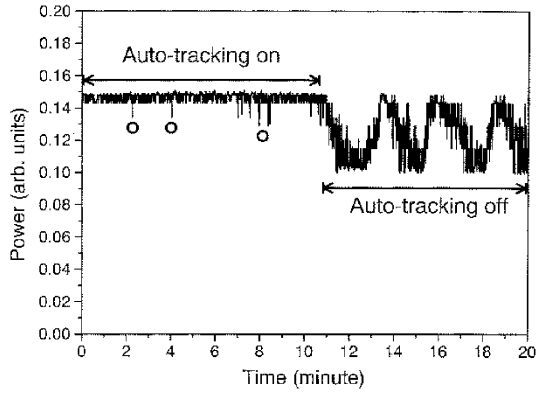

Fig. 10. Long-term monitoring of the output power fluctuations of the Brillouin fiber laser, showing the stabilizing effect of the tracking feedback control.

variation in the cavity was the most significant contributor to the remaining laser-power fluctuation. The pump-power variation was believed to be mainly due to the interference effect of pump light in the resonator cavity resulting from the imperfect transmission characteristic of the UMZI.

The negative peaks marked by circles in the Fig. 10 are supposed to be due to abrupt change of pump LD frequency originating from the noise of temperature controller and environmental perturbations. In fact, the pump LD frequency could be varied up to a few tens MHz in the worst case. However, one can observe that the efficient operation of the autotracking circuit makes the laser-output power immediately recover the maximum value. When the autotracking was turned off, the laser power began to severely fluctuate over more than 33%. For a more stable laser output, the pump LD and the laser cavity must be controlled more accurately, and a higher extinction ratio UMZI is needed.

IV. Conclusion

We have demonstrated a novel Brillouin fiber laser using an unbalanced MZ interferometer and we have described in detail the basic operation of such a laser. This configuration aims at offering a stable single-frequency BFL while pumped by a conventional DFB LD. The need for cavity resonance matching of the pump is intrinsically absent of such a configuration. The BFL operates predominantly in a single longitudinal mode with a linewidth measured to be below 0.94 kHz. This demonstrates the excellent spectral purity that may be achieved with a BFL. With a simple power-stabilization circuit based on dithering and autotracking method, the power drift and fluctuation were reduced to 4%. This laser can find applications such as linewidth-narrowing of standard DFB lasers and sensors based on conventional Brillouin fiber-ring lasers, with the crucial advantage of overcoming the necessity of a critically coupled resonator.

Acknowledgment

The authors would like to thank K. Y. Song, KAIST Fiber-Optics Laboratory, Taejon, Korea, for providing the fused-fiber couplers. They are also grateful to M. Facchini, P. S. Ennabli, and F. Briffod, EPFL Laboratory of Metrology and Photonics, Lausanne, Switzerland, for their support and fruitful discussions.

References

[1] G. P. Agrawal, *Nonlinear Fiber Optics*, 2nd ed. San Diego, CA: Academic, 1995, pp. 370–403.
[2] A. R. Chraplyvy, "Limitations in lightwave communications imposed by optical-fiber nonlinearities," *J. Lightwave Technol.*, vol. 10, pp. 1548–1557, 1990.
[3] P. Labudde, P. Anliker, and H. P. Weber, "Transmission of narrow band high power laser radiation through optical fibers," *Opt. Commun.*, vol. 32, pp. 385–390, 1990.
[4] T. C. Rich and D. A. Pinnow, "Evaluation of fiber optical waveguides using Brillouin spectroscopy," *Appl. Opt.*, vol. 13, pp. 1376–1378, 1974.
[5] M. Ohashi, N. Shibata, and K. Shiraki, "Fiber diameter estimation based on guided acoustic wave Brillouin scattering," *Electron. Lett.*, vol. 28, pp. 900–902, 1992.
[6] T. Horiguchi and M. Tateda, "Optical-fiber-attenuation investigation using stimulated Brillouin scattering between a pulse and a continuous wave," *Opt. Lett.*, vol. 14, pp. 408–410, 1989.
[7] M. Tateda, T. Horiguchi, T. Kurashima, and K. Ishihara, "First measurement of strain distribution along field-installed optical fibers using Brillouin spectroscopy," *J. Lightwave Technol.*, vol. 8, pp. 1296–1272, 1990.
[8] T. Kurashima, T. Horiguchi, and M. Tateda, "Distributed temperature sensing using stimulated Brillouin scattering in optical silica fibers," *Opt. Lett.*, vol. 15, pp. 1038–1040, 1990.
[9] M. F. Ferreira, J. F. Rocha, and J. L. Pinto, "Analysis of the gain and noise characteristics of fiber Brillouin amplifiers," *Opt. Quantum Electron.*, vol. 26, pp. 34–44, 1994.
[10] K. Kalli, D. O. Culverhouse, and D. A. Jackson, "Fiber frequency shifter based on generation of stimulated Brillouin scattering in high-finesse ring resonator," *Opt. Lett.*, vol. 16, pp. 1538–1540, 1991.
[11] D. Culverhouse, K. Kalli, and D. A. Jackson, "Stimulated Brillouin scattering ring resonator laser for SBS gain studies and microwave generation," *Electron. Lett.*, vol. 27, pp. 2033–2035, 1991.
[12] K. O. Hill, D. C. Johnson, and B. S. Kawasaki, "CW generation of multiple Stokes and anti-Stokes Brillouin-shifted frequencies," *Appl. Phys. Lett.*, vol. 29, pp. 185–187, 1976.
[13] L. F. Stokes, M. Chodorow, and H. J. Shaw, "All-fiber stimulated Brillouin ring laser with sub-milliwatt pump threshold," *Opt. Lett.*, vol. 7, pp. 509–511, 1982.
[14] S. P. Smith, F. Zarinetchi, and S. Ezekiel, "Narrow-linewidth stimulated Brillouin fiber laser and applications," *Opt. Lett.*, vol. 16, pp. 393–395, 1991.
[15] F. Zarinetchi, S. P. Smith, and S. Ezekiel, "Stimulated Brillouin fiber-optic laser gyroscope," *Opt. Lett.*, vol. 16, pp. 229–231, 1991.
[16] J. Boschung, L. Thévenaz, and P. A. Robert, "High-accuracy measurement of the linewidth of a Brillouin fiber ring laser," *Electron. Lett.*, vol. 30, pp. 1488–1489, 1994.
[17] M. Niklès, L. Thévenaz, and P. A. Robert, "Brillouin gain spectrum characterization in single-mode optical fibers," *J. Lightwave Technol.*, vol. 15, pp. 1842–1851, 1997.
[18] R. Carrol, C. D. Coccoli, D. Cardarelli, and G. T. Coate, "The passive resonator fiber optic gyro and comparison to the interferometer gyro," *Proc. SPIE*, vol. 719, pp. 169–177, 1986.
[19] P. Bayvel and I. P. Giles, "Evaluation of performance parameters of single-mode all-fiber Brillouin ring lasers," *Opt. Lett.*, vol. 14, pp. 581–583, 1989.
[20] G. J. Cowle, D. Y. Stepanov, and Y. T. Chieng, "Brillouin/erbium fiber lasers," *J. Lightwave Technol.*, vol. 15, pp. 1198–1204, 1997.
[21] A. Küng, P.-A. Nicati, and P. A. Robert, "Reciprocal and quasireciprocal Brillouin fiber-optic current sensor," *IEEE Photon. Technol. Lett.*, vol. 8, pp. 1680–1682, 1996.
[22] Y. Tanaka and K. Hotate, "Analysis of fiber Brillouin ring laser composed of single-polarization single-mode fiber," *J. Lightwave Technol.*, vol. 15, pp. 838–844, 1997.
[23] P.-A. Nicati, K. Toyama, and H. J. Shaw, "Frequency stability of a Brillouin fiber ring laser," *J. Lightwave Technol.*, vol. 13, pp. 1445–1451, 1995.
[24] A. Küng, L. Thèvenaz, and P. A. Robert, "Polarization analysis of Brillouin scattering in a circularly birefringent fiber-ring resonator," *J. Lightwave Technol.*, vol. 15, pp. 977–982, 1997.
[25] M. O. Deventer and A. J. Boot, "Polarization properties of stimulated Brillouin scattering in single-mode fibers," *J. Lightwave Technol.*, vol. 12, pp. 585–590, 1994.

[26] P.-A. Nicati, K. Toyama, S. Huang, and H. J. Shaw, "Temperature effects in a Brillouin fiber ring laser," *Opt. Lett.*, vol. 18, pp. 2123–2125, 1993.
[27] P. B. Gallion and G. Debarge, "Quantum phase noise and field correlation in single frequency semiconductor laser systems," *IEEE J. Quantum Electron.*, vol. QE-20, pp. 343–349, 1984.

Luc Thévenaz (M'02) received the M.Sc. degree in astrophysics from the Observatory of Geneva, Geneva, Switzerland, in 1982 and the Ph.D. degree in physics from the University of Geneva, Geneva, Switzerland, in 1988, where he developing his field of expertise, namely, fiber optics.

In 1988, he joined the Swiss Federal Institute of Technology of Lausanne (EPFL), Switzerland. In 1991, he visited the PUC University, Rio de Janeiro, Brazil, and Stanford University, Stanford, CA, where he participated in the development of a Brillouin laser gyroscope. In 1998 and 1999, he stayed at the Korea Advanced Institute of Science and Technology (KAIST), Daejon, South Korea, where he worked on fiber laser current sensors. In 2000, he cofounded the spin-off company Omnisens, which is developing and commercializing advanced photonic instrumentation. Currently, he leads a research group at the EPFL that is involved in photonics, in particular, fiber optics and optical sensing. Research topics include electrical current fiber sensors, Brillouin-scattering fiber sensors, fiber nonlinearities measurement techniques, and laser-diode spectroscopy of gases.

Jae Chul Yong, photograph and biography not available at the time of publication.

Byoung Yoon Kim (S'83–M'85–SM'92–F'99), photograph and biography not available at the time of publication.